THE NUMERICAL SIMULATION AND EXPERIMENTAL MEASUREMENT OF A SCALED AHMED BODY MODEL WITH MODIFIED GEOMETRY

KATERINA ANDRLOVA[1]

[1]Department of Vehicles and Engines, Faculty of Mechanical Engineering, Technical University of Liberec, Liberec, Czech Republic

In this work, the aerodynamic analysis of the original and modified Ahmed body was done. The principle of modification was the chamfer angle on the back sides of the Ahmed body like a boat tail, which was expected to decrease the magnitude of the drag force. The value of the aerodynamic coefficients was carried out using CFD modelling and data were validated in wind tunnel measurements. For those measurements, it was necessary to design simple aerodynamic balances, since the utilized wind tunnel was not equipped with any. It has been expected that the drag force coefficient of the modified model should be reduced compared to original geometry.

1 INTRODUCTION

Nowadays, automotive aerodynamics is playing one of the most important roles in the vehicle design process. Since the requirements for emissions of greenhouse gasses are becoming stricter, it is getting harder to fulfill those requirements. One way to reduce fuel consumption is to improve the combustion process, another way is reducing the drag force of the vehicle. In literature, [Hucho 1990], we can find the information that at speed of 100 km/h almost 80 % of total engine power is being consumed to overcome the drag force. The magnitude of the aerodynamic forces is directly proportional to the square of the velocity and the magnitude of power needed to overcome drag force is proportional to the cube of the velocity. This also applies to other aerodynamic forces (lift force, side force), which influence for example the stability of a vehicle and therefore traffic safety, [Hucho 1993]. There are more types of drag force, depending on how this drag is generated. There is a pressure (profile drag), which is caused by the separation of the boundary layer and from the wake, a skin friction drag, caused by viscosity of the fluid and the surface quality of the object, the interference drag, the induced drag and the cooling drag. The greatest part of its magnitude comes from the pressure drag, that is about 60 %, [Hucho 1993].

Because there is a huge expansion of Computational Fluid Dynamics (CFD) in the last twenty years, it has also registered a massive development of utilization in automotive aerodynamics. Since the CFD is quite cheap (compared to the experimental methods) and also is becoming more precise than ever before, it is playing a major role in the first stage of the design process. Nowadays, the CFD is used for comparing several designs and choosing the optimal one, calculating approximate values of aerodynamic forces, momentum, pressure, velocity etc. But it is still limited in the mesh size and CPU, also in accuracy. Also, it is important to evaluate whether the results are corresponding with reality.

In the automotive design process, it is important to account for the interference of the flow. This also means that every change in geometry can result in completely different consequences of the resulting flow field. Hence there are several simplified car models, which are widely used in simulations to test the geometry changes. There is a SAE model [Hetawal 2014], Davis model [Mansor 2015], DrivAer model [Gerlicher 2013], Mira [Zhang 2019] etc. But the best known and most widely used simplified car model is the Ahmed body, [Ahmed 1984], which geometry configuration with 30° slant angle is shown in Figure 1. As it can be seen in the picture, the Ahmed body can be divided into three parts: a fore body with rounded edges, a box shaped middle section with rectangular cross section and the rear end with slant, with length of 222 mm and slant angles between 0° to 40°. In Figure 1, the variant with 30° slant angle is depicted, because this variant has been used in this work. From [Ahmed 1984] follows, that nearly 85 % of the total drag is pressure drag and the forebody contributes at most 9 % to the total value of pressure drag and the rest is generated by the rear end.
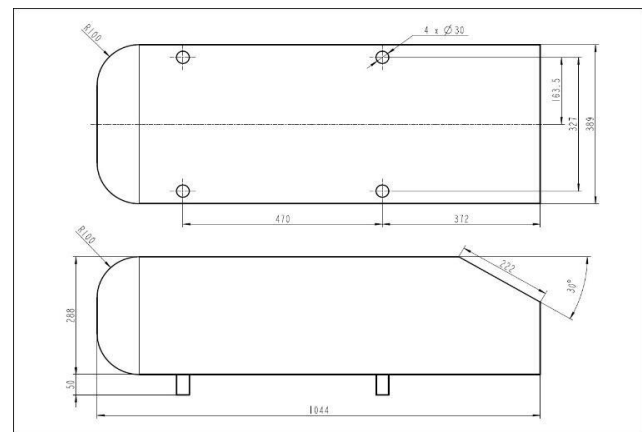
Figure 1 The original Ahmed body geometry with 30° slant angle

Since the success of the Ahmed body, there has been many studies with geometry modification made. In studies [Buscariolo 2021], [Aulakh 2016], [Mb 2018], [Moghimi 2018], the Ahmed body has been equipped with underbody diffuser and the influence of the diffuser angle or the length has been studied. In the study of [Mb 2018], the value of the diffuser angle for the minimum drag was find to be 12°. In the work of [Buscariolo 2021], there were two original Ahmed body geometries studied. First with the 0° and the second with the 25° slant angle. The diffuser angle varied between 10° to 50° in increment of 10°. The case with 25° slant angle observed the drag reduction in cases with the diffuser angles up to 20°, while the downforce was increasing.

The study [Govardhan 2023] was focused on the adjoint shape optimization which was made for 30° slant angle Ahmed body and there was 7 to 10 % drag reduction achieved.

The work of [Muñoz-Hervás 2024] is studying experimentally the influence of rear vertical flexible and rigid flaps and its interaction with the wake behind the Ahmed body with the dimensions H x W x L= 72mm x 290,88mm x 97,2mm. The effect of the flap can be similar to a boat tail shape. The study also

examines the influence of the crosswind. From this study, it can be found, that the flap deflection angle of 4° can lead to 8,3 % decrease in the global drag.

Another shape modification has been studied in a work of [Siddiqui 2023], where the 1:4 scaled-down Ahmed body with 25° slant angle and elliptical slant surface has been proposed. For the simulations, IDDES model (hybrid model of the DDES and Wall Modeled Large Eddy simulation) has been used. For 25° slant angle and low Reynolds number, the value of drag coefficient was reduced of 6,6 % and for the high Reynolds number case, the drag value decreased by 10,4 %.

The effect of deflectors on the aerodynamic drag has been examined in the work of [Hung Tran 2023]. The maximum drag reduction of 8 % has been observed for 0° deflection angle.

In previous studies, the influence of shape modifications (underbody diffusor, rear side flaps, elliptical shape, etc.) of Ahmed body was studied. This study is going to focus on another shape modification, the chamfer of the back sides (boat-tail like), and is going to evaluate the change in the drag coefficient.

2 COMPUTATIONAL MODEL

Since the main increment to the drag force is created by the rear side of the body (and its wake structure), it was supposed that another variation in arrangement of the rear end should result in the reduction of the total drag force. In this study, the rear sides of the Ahmed body have been chamfered like a boat tail, as can be seen in Figure 3. The value of the angle of chamfer varies between the value of 0° (original Ahmed body) and 25° with step of 5°. Bigger value than 25° was not considered, because the utility volume of the rear end (we are still thinking about Ahmed body as a car) would decrease too much. It can be seen that the size of the side chamfer is 222 mm, so it is of the same size as the Ahmed bodie's slant dimension.

The software Ansys Fluent TM has been used for the numerical simulations. Because the flow field around the Ahmed body is considered to be incompressible, stationary and turbulent, the RANS k-ε realizable model with non-equilibrium wall-functions was chosen. Name RANS comes from Reynolds-Averaged Navier-Stokes Equations, what means, that in the equation for any turbulent quantity U, there is a part for average value $\overline{U}$ and part for fluctuating value, denoted by u', like:

$$U = \overline{U} + u' \tag{1}$$

Original k-ε model has relatively good results in simulations of free stream but struggles in the near wall region. But its modification k-ε realizable solves this problem and therefore this model is commonly used in automotive industry simulations for its simplicity and low CPU cost.

k-ε turbulence model is semi-empiric two equational model whose model constants are set empirically. One equation is for turbulent energy k and the second one for dissipation ε. Turbulent viscosity is defined as [Chung 2002]:

$$\mu_t = C_\mu \rho \sqrt{k} L = C_\mu \rho \frac{k^2}{\varepsilon} \tag{2}$$

Where L is the length scale and ρ is the density. The equation for turbulent transport of energy is:

$$\frac{\partial(\rho k)}{\partial t} + \frac{\partial(\rho \widetilde{U_j} k)}{\partial x_j} = P_k + \frac{\partial}{\partial x_j}\left[\left(\mu + \frac{\mu_t}{\sigma_k}\right)\frac{\partial k}{\partial x_j}\right] - \rho \varepsilon \tag{3}$$

and can be transformed to:

$$\frac{\partial(\rho \varepsilon)}{\partial t} + \frac{\partial(\rho \widetilde{U_j} \varepsilon)}{\partial x_j} = \frac{\varepsilon}{k} C_{\varepsilon 1} P_k + \frac{\partial}{\partial x_j}\left[\left(\mu + \frac{\mu_t}{\sigma_\varepsilon}\right)\frac{\partial \varepsilon}{\partial x_j}\right] - \frac{\varepsilon}{k} C_{\varepsilon 2} \rho \varepsilon \tag{4}$$

where P_k is a production of turbulent energy. Therefore, there are 5 empirical constants in this model: C_μ, σ_k, σ_ε, $C_{\varepsilon 1}$ and $C\varepsilon 2$. These constants can be determined from experimental data of simpler flows or by numerical optimization. Typical values of those constants are: C_μ=0,09, σ_k=1,0, σ_ε=1,3, $C_{\varepsilon 1}$=1,44 a $C_{\varepsilon 2}$=1,92, [Prihoda 2007]. Basic version of the k-ε model is appropriate only for flow in sufficient distance from the wall, where the value of the Reynolds number is sufficiently high. In the near wall region, fluctuations of the velocity perpendicular to the wall are more damped. Then, the turbulence is not of isotropic character and the basic versions of the model are not suitable for description of the flow field. In order to resolve that problem, newer versions of the k-ε model were developed, for example the k-ε *Realisable* model, which has been used in this work.

Nonequilibrium wall functions (NWF) are taking into account variations in the thickness of viscous sublayer and are more realistic in estimation of turbulent behaviour in the boundary layer without prolonging the computational time.
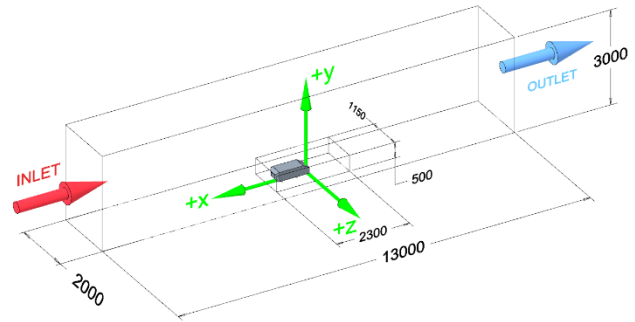
Figure 2 The computational domain
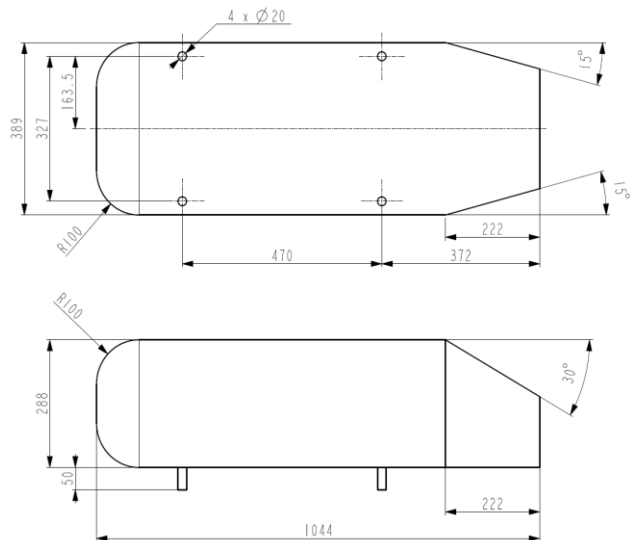
Figure 3 Modified Ahmed body with 15° side chamfer, [Andrlova Katerina 2023]

The computational domain has a total length 1300 mm, a width 2000 mm and height 3000 mm and is depicted in Figure 2. In this picture can be also seen that there is also a smaller refinement volume in the closer region of the Ahmed body, which provides more subtle mesh. Maximum mesh skewness was 0,61 and average skewness was 0,189. The boundary conditions are

summarized in Table 1. The inlet velocity was in the first case 40 m/s.

The final element count for the model was about 7 million. The structure of the mesh was tetrahedral, with refinement in the vicinity of the body and in the wake region. On the surface of the body and on the ground region, a prism layer mesh with 6 layers was sized to model the near wall boundary layer. The mesh is depicted in Figure 4.
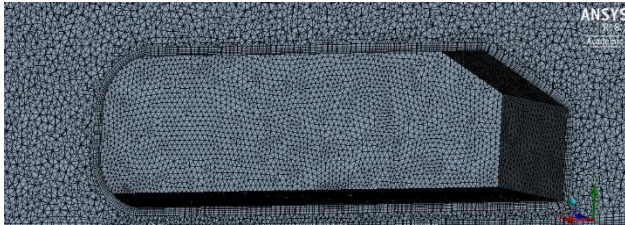
Figure 4 Detailed mesh

Inlet	v=40 m/s turbulence intensity 1 %
Outlet	turbulence intensity 5 %
Ahmed Body	no-slip condition with non-equilibrium wall functions
Ground	no-slip condition with non-equilibrium wall functions
Walls of the wind tunnel	no-slip condition with non-equilibrium wall functions

Table 1 The boundary conditions for the numerical simulations

From those first simulations can be seen, that the value of the drag coefficient c_D and lift coefficient c_L is decreasing with the increase of the chamfer angle till the size of the chamfer angle about 15°, where the value of the drag coefficient remains limited, Figure 5. From the first simulations, the value of 15° chamfer angle has been chosen to be the best one, because another increase of the chamfer would only lead to the decrease of the utility volume of the body.
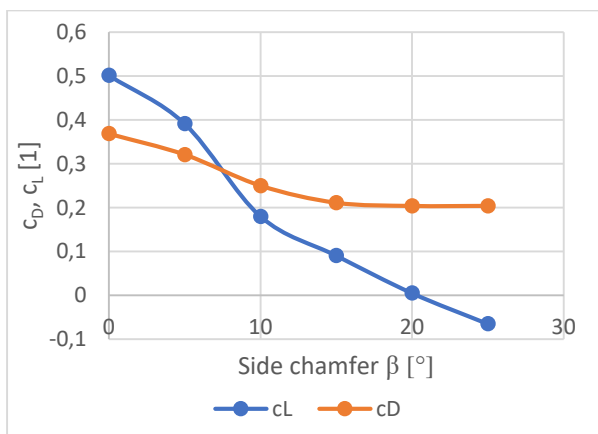
Figure 5 Drag and lift coefficients for the different side chamfer angles

In the second step, it has been worked only with two variants, the original Ahmed body geometry and the "optimal" one, with the 15° chamfer angle. It was necessary to validate the results experimentally. Since the university wind tunnel has only a small test section, it was essential to use 1:10 scaled models. Due to [Pope et al. 1966], when it is not possible to measure at the precise velocity, it is conceivable to measure the value of forces (and to calculate the value of force coefficient) for several velocities and then to interpolate a curve through these values and get the dependence of the force coefficient on the velocity. In this study, the measurements were conducted at the velocities in the wind tunnel from 5 to 40 m/s with the increase of 5m/s by each measurement and the values were measured every 5 m/s difference. All the measurement settings were simulated for both body cases, original and 15° chamfer angle, in Ansys Fluent for the scale 1:10 of the model and then measured practically in the wind tunnel.

3 EXPERIMENTAL VALIDATION

The experimental tests were conducted in the laboratory of CXI at the Technical University of Liberec. The wind tunnel was a closed circuit with a closed test section. The test section dimensions were (W x H x L) 200 mm x 200 mm x 480 mm.

Free stream turbulence intensity of the wind tunnel was 1 %. A chosen sampling frequency was 600Hz.

The wind tunnel could provide velocities up to 40 m/s. Since the size of the section was small, therefore the 1:10 scaled model was used and so it was necessary to make simulations for two scaled models (0° chamfer and the optimal geometry modification with 15° chamfer) and for velocities from 5 to 40 m/s with the step of 5 m/s to get the dependency of the drag coefficient on the velocity.

The value of the Reynolds number *Re* can be calculated from the relation:

$$Re = \frac{U_\infty \cdot l}{\nu} \tag{5}$$

Where U_∞ is the free stream velocity, *l* is the characteristic dimension (the length of the Ahmed body) and ν is the kinematic viscosity. For the first case (search for the dependence of the drag and lift coefficients on the chamfer angle), where the Ahmed body was in its original size (1044 mm) and the velocity was fixed at 40 m/s, the value of the Reynolds number was approximately 2 763 000. The value of the velocity in experimental validation varied between 5 to 40 m/s with increment of 5 m/s, the length of the scaled model was 0,1044 m and the kinematic viscosity was 15,11 ·10⁻⁶ m²/s, so the resulting value of the Reynolds number varied approximately between 34 500 and 276 300, therefore the biggest Reynolds number was 10 times smaller than the Reynolds number in the simulation case in part 2.

Figure 6 Wind tunnel with the mounted model and measuring equipment

Since the wind tunnel was not equipped with aerodynamic balance, it was necessary to design and assemble one. Because it was crucial to measure the drag force (the primary objective of this work is to reduce the drag force), this balance system was designed just to measure the drag force (and not the other forces and moments), as can be seen in the Figures 6 and 7.

To simulate the ground effect, the model was mounted to the ground of the wind tunnel test section. In order to reduce the influence of the balance system, the whole balance system was placed outside of the wind tunnel, under the test section.
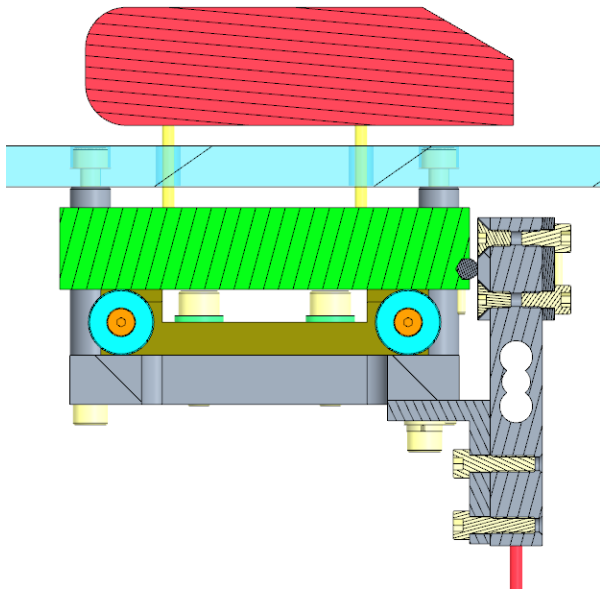
Figure 7 Scheme with the mounted model and measuring equipment

4   RESULTS

From the wind tunnel experiment, the magnitudes of the forces have been obtained and it was necessary to calculate the drag coefficient. The value of the drag coefficient c_D has been calculated by:

$$c_D = \frac{F_x}{1/2 \cdot \rho \cdot A \cdot U_\infty^2} \tag{6}$$

Where F_x is the value of the drag force measured, ρ is the value of the air density (for measurement conditions in the wind tunnel ρ=1,1845 kg/m³), A is the area of the frontal projection of the Ahmed body and U_∞ is the velocity of the free stream.

The results for the scaled 1:10 model from experimental measurements and from the simulations are depicted in Figures 8 and 9. For the 0° chamfer (the original Ahmed body geometry) applies, that the bigger the velocity (Reynolds number) is, the smaller the drag coefficient. For the 15° chamfer case applies, that the drag coefficient drops with the growth of the velocity until the 15 m/s (Re≈103 640) where the slope of the curve gets smaller in simulation or almost constant in the experimental one.

In Figure 10, there are drag coefficients differences of the original and 15° chamfer geometry for experimental data (marked with blue) and for the simulations (marked with orange). For the chamfer angle of 5°, the value of the drag coefficient is smaller only by approximately 6 % for simulation or experimental case respectively. For the increase of the velocity (or the Reynolds number), the drag coefficient difference of original and 15° chamfer is increasing for experiment and

simulation both till the value of 15 m/s for experimental evaluation or 20 m/s for simulation, when the drag coefficient difference starts to decrease, as can be seen in the Figure 10. The maximum drag coefficient drop of 31 % was observed in the case of 15 m/s (Re≈103 640) for the experiment and approximately 34 % in the case of 20 m/s (Re≈138 190) for the simulation case. It is difficult to identify the reason in difference between experimental and numerical results, but it can be caused by the limitations of the CFD simulations or due to inaccuracy of measurements.
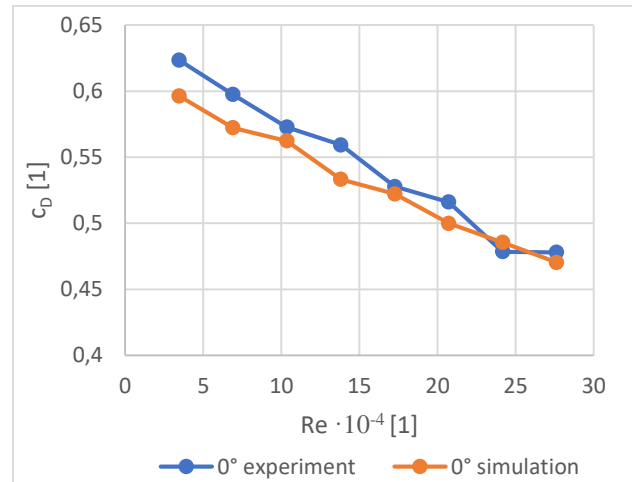
Figure 8 Comparison of results from experimental measurements in wind tunnel and simulations for 0° chamfer
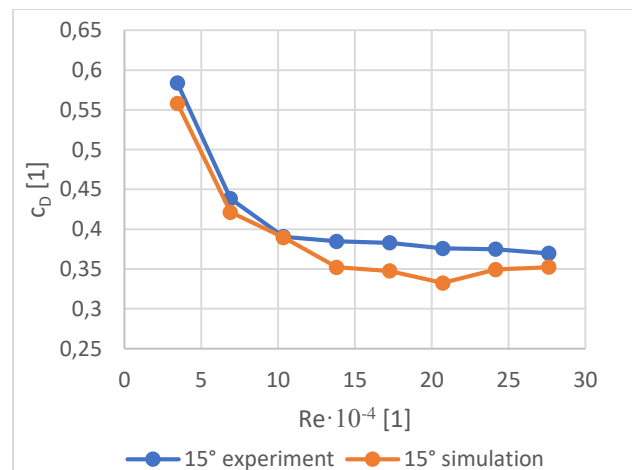
Figure 9 Comparison of results from experimental measurements in wind tunnel and simulations for 15° chamfer

As it was said before, the main contribution to the drag force comes from the wake structure. As can be seen in Figure 11 and Figure 12, the wake structure from the original geometry is much wider than the wake structure of the modified geometry. The reason for this is, that the boat tail shape helps the flow to accelerate on the back sides of the body (similar to airfoil, where the suction upper part has longer surface than the lower part and therefore the velocity of the flow is bigger on the upper side) and therefore to bring the energy to the wake field.
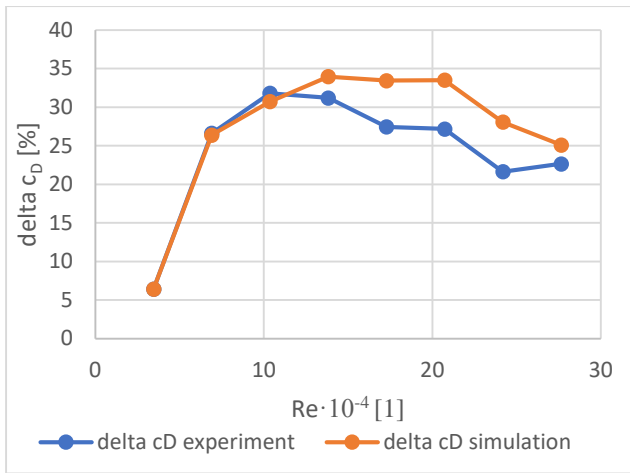
Figure 10 Drag coefficient decrease in percentage of the 0° chamfer case with the increase of the Reynolds number for experimental/ simulation case respectively
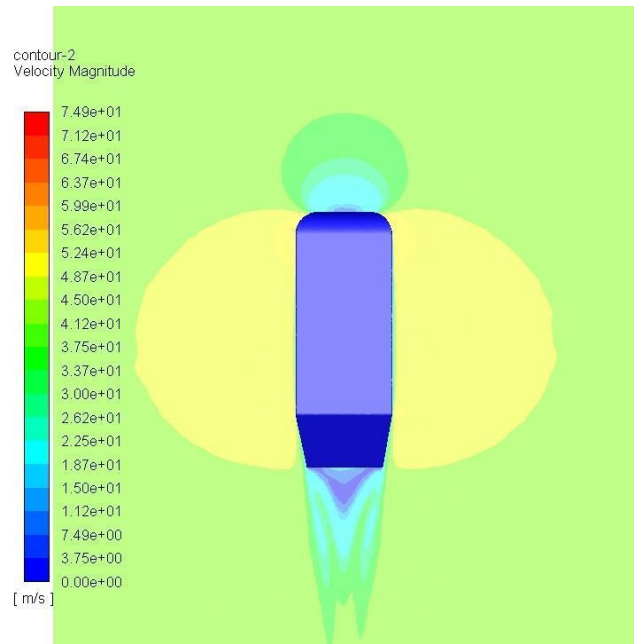
Figure 12 Velocity field for the modified Ahmed body with 15° chamfer angle at velocity 40 m/s
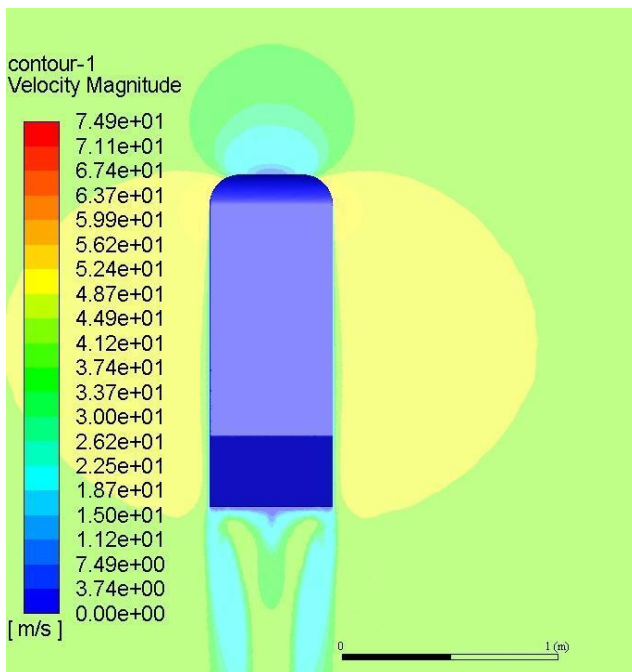
Figure 11 Velocity field for the 0° chamfer Ahmed body at the velocity 40 m/s

Figure 13 Velocity field for the scaled 0° chamfer Ahmed body at the velocity 40 m/s

In Figures 13 and 14, the velocity flow filed form the side view in the symmetry plane is depicted. The main difference can be found in the wake field, as expected. The wake height for the 15° chamfer is higher than in the case of 0° chamfer. This could be caused due to the flow coming from the chamfered sides, which is interacting with the flow from the slanted back upper surface.
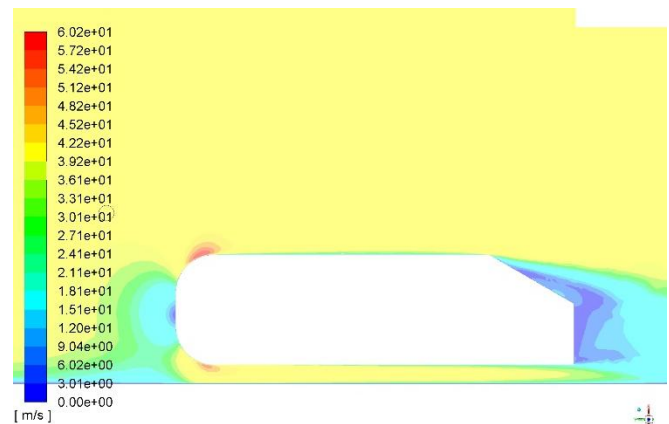
Figure 14 Velocity field for the scaled 15° chamfer Ahmed body at the velocity 40 m/s

5 CONCLUSION

The objective of this work was to examine the consequence of the shape modification consisting of the chamfer of the back sides of the Ahmed body onto the magnitude of the drag coefficient. In this work, it has been shown that the chamfer of the back sides of the Ahmed body improves the flow field and especially the wake field and therefore is capable of decreasing the lift and the drag coefficients. From the simulations done for the original size model, it comes out, that for the velocity 40 m/s and 15° chamfer angle, the value of the drag coefficient decreased by 45 % and the value of the lift force decreased by 80 % compared to the original geometry values.

The experimental measurement confirms the influence of the shape modification on the magnitude of the drag force. From the experiment, the biggest difference, almost 31 %, between the original and modified scaled model, was recorded for the velocity of 15 m/s for the experimental data, or for the simulation results, where the biggest difference was observed for the velocity 20 m/s and it was approximately 34 %.

From the simulations and measurements, it can be said that the boat tail shape can reduce the value of the drag force (and from simulations also the lift force). This means that the boat tail-like geometry modification of the Ahmed body would therefore decrease the fuel consumption or the electricity consumption for electric vehicles (and therefore the emissions of CO_2). This modification would also improve the stability of the vehicle, because of the drop of the lift force and therefore contribute to traffic safety. However, it is necessary to highlight, that those results are valid only for scaled 1:10 Ahmed body (simplified geometry and smaller Reynold numbers) and in case of the actual car, due to interference of the flow, could lead to less favourable results.

REFERENCES

[Ahmed 1984] Ahmed, S. R., et al. Some Salient Features of the Time -Averaged Ground Vehicle Wake. SAE Transactions. 1984, Vol. 93, pp. 473–503. ISSN 0148-7191

[Andrlova 2023] Andrlova, K. The Numerical Simulation of Ahmed Body with Modified Geometry. Scientific Proceeding KOKA 2023, p. 7 pages. Hustopece u Brna : VUT Brno. 6th September 2023. ISBN 978-80-214-6164-2.

[Aulakh 2016] Aulakh, D. J. S. Effect of underbody diffuser on the aerodynamic drag of vehicles in convoy. PHAM, Duc (ed.), Cogent Engineering. 2016 Vol. 3, no. 1, p. 1230310. DOI 10.1080/23311916.2016.1230310.

[Buscariolo 2021] Buscariolo, F. et al.. Computational study on an Ahmed Body equipped with simplified underbody diffuser. Journal of Wind Engineering and Industrial Aerodynamics. 2021 Vol. 209, p. 104411. DOI 10.1016/j.jweia.2020.104411.

[Chung 2002] Chung, T. J. Computational Fluid Dynamics. Cambridge: Cambridge University Press, 2002. ISBN 9780511606205

[Delassaux 2021] Delassaux, F. et al. Sensitivity analysis of hybrid methods for the flow around the ahmed body with application to passive control with rounded edges. Computers & Fluids. 2021 Vol. 214, p. 104757. DOI 10.1016/j.compfluid.2020.104757.

[Frank 2013] Frank, T., et al. DrivAer-Aerodynamic Investigations for a New Realistic Generic Car Model using ANSYS CFD. October 2013, Automotove Simulation World Congress, Frankfurt am Main, Germany

[Govardhan 2023] Govardhan, D. et al. Adjoint shape optimization of Ahmed body to improve aerodynamics. Materials Today: Proceedings. 2023 DOI 10.1016/j.matpr.2023.06.410.

[Hetawal 2014] Hetawal, S. et al. Aerodynamic Study of Formula SAE Car. Procedia Engineering. 2014. Vol. 97, pp. 1198–1207. ISSN 1877-7058

[Hucho 1990] Hucho, W. H. Aerodynamics of Road Vehicles. Great Britain: Butterworth-Heinemann, 1990. ISBN 0-408-01422-9.

[Hucho 1993] Hucho, W. H. and Sovran, G. Aerodynamic of Road Vehicles. General Motors Research and Enviromental Staff, Michigan, 1993. Annual review.

[Hung Tran 2023] Hung Tran, T. et al. Surface flow and aerodynamic drag of Ahmed body with deflectors. Experimental Thermal and Fluid Science. 2023 Vol. 145, p. 110887. DOI 10.1016/j.expthermflusci.2023.110887.

[Mansor 2015] Mansor, S. et al. Validation of CFD Modeling and Simulation of a Simplified Automotive Model. Applied Mechanics and Materials. 2015, Vol. 735, pp. 319–325. DOI 10.4028/www.scientific.net/AMM.735.319.

[Mb 2018] MB, A., et al. 2018. Parametric Investigation of Effect of Diffuser Angle on the Flow Characteristics of an Ahmed Body. International journal of engineering research and technology 2018 [online].

[Moghimi 2018] Moghimi, P. and Rafee, R. Numerical and Experimental Investigations on Aerodynamic Behavior of the Ahmed Body Model with Different Diffuser Angles. Journal of Applied Fluid Mechanics. 2018 Vol. 11, pp. 1101–1113. DOI 10.29252/jafm.11.04.27923.

[Muñoz-Hervas 2024] Muñoz-Hervas, J.C. et al. Experimental investigation of rear flexible flaps interacting with the wake dynamics behind a squareback Ahmed body. Journal of Fluids and Structures. 2024 Vol. 127, p. 104124. DOI 10.1016/j.jfluidstructs.2024.104124.

[Pope 1966] Pope, A., et al. Low Speed Wind Tunnel Testing 3. New York: John Wiley & Sons, 1966. ISBN 978-0-471-55774-6.

[Prihoda 2007] Prihoda, J. and Louda, P. Mathematical Modelling of Turbulent Flow. Prague: CTU in Prague, 2007. ISBN 978-80-01-03623-5.

[Siddiqui 2023] Siddiqui, N. A. and Agelin-Chaab, M. Investigation of the wake flow around the elliptical Ahmed body using detached Eddy simulation. International Journal of Heat and Fluid Flow. 2023 Vol. 101, p. 109125. DOI 10.1016/j.ijheatfluidflow.2023.109125.

[Zhang 2019] Zhang, Y. et al. Aerodynamic Characteristics of Mira Fastback Model in Experiment and CFD. International Journal of Automotive Technology, 2019, Vol. 20, No. 4, pp. 723–737. ISSN 1976-3832

CONTACTS:

Ing. Katerina Andrlova
Technical university of Liberec, Departement of Vehicles and Engines
Studentska 1402/2, Liberec, 461 17, Czech Republic
+420 776 042 271, katerina.andrlova@tul.cz, https://kvm.tul.cz/cs/zamestnanec/ing-katerina-andrlova